

**MECHANISM OF NEAR-INFRARED  
FLUORESCENT SIGNAL GENERATION IN  
PROTEOLYSIS-SENSITIVE MACROMOLECULAR  
IMAGING PROBES**

A Major Qualifying Project Report  
submitted to the faculty of the  
WORCESTER POLYTECHNIC INSTITUTE  
in partial fulfillment of the requirements for the  
degree of Bachelor of Science in  
Biology and Biotechnology

Submitted by:

---

Jessica C. López

April 25, 2013

APPROVED:

---

Alexei Bogdanov, Ph.D. Sc.D.  
Department of Radiology  
UMass Medical School  
MAJOR ADVISOR

---

David Adams, Ph.D.  
Biology and Biotechnology  
WPI Project Advisor

## Abstract

*In vivo* optical imaging of proteolysis in inflammatory and tumor microenvironments can be monitored through excitable fluorophore-labeled, long-circulating probes using a graft copolymer of poly(ethylene glycol) and poly-L-lysine as a carrier molecule. In this project, both *in vitro* and cell culture experiments were performed to investigate the major mechanisms of PGC-fluorophore probe cleavage via stromal cell proteases (i.e. time-dependent changes in fluorescence intensity of the intracellular compartment and changes of cyanine dye fluorescence lifetimes of the probes). It was observed that trypsin-mediated cleavage of PGC-fluorophore probes results in distinct fragment sizes as measured by gel electrophoresis, a 2-fold increase in fluorescence intensity, and a rapid 1.5-fold increase in fluorescence lifetime. Finally, it was observed that human squamous carcinoma cells uptake PGC-fluorophore probes faster than normal human dermal fibroblasts with a greater fluorescence intensity over time.

## **Table of Contents**

Abstract .....	2
Table of Contents .....	3
Acknowledgements .....	4
Background .....	5
Project Purpose .....	15
Materials & Methods .....	16
Results .....	20
Discussion .....	28
Bibliography .....	32
Appendix .....	34

## **Acknowledgements**

I would like to extend my utmost gratitude to Dr. Alexei Bogdanov for his support and guidance throughout this project, and for affording me the opportunity to be a part of his lab at the University of Massachusetts Medical School. I would also like to thank Dr. Suresh Gupta and Dr. Surong Zhang for their time and assistance helping me with various lab skills and techniques. Lastly, I would like to thank Prof. David Adams for his guidance and insight on the project. I am grateful for Dr. Bogdanov's and Prof. Adam's assistance with the final report.

# 1 Background

## 1.1 Disease-associated Enzymatic Activity

The detection of enzymatic activity in cells and tissues has proven to be beneficial in the diagnosis and prognosis of a variety of diseases. There is substantial evidence that deregulation of enzymatic activity results in the etiology and progression of cancer, atherosclerosis, multiple sclerosis, Alzheimer's disease, and various infections. Specifically in cancers, proteases have been observed to have distinct roles in tumor growth, invasion, migration, and angiogenesis (Koblinski et al, 2000). Proteases, such as matrix metalloproteinases (MMPs), have been noted to facilitate extracellular matrix breakdown, which allows cancer cells to invade neighboring tissues along with activated stromal cells. Deregulation of MMPs is expressed at different levels of tumorigenesis, invasiveness, metastasis, and degree of tumor vascularization (Pengfei et al., 2012). Other proteases such as cysteine proteases (i.e. cathepsins) have increased expression levels in tumor microenvironments. Cathepsin B is a lysosomal protease associated with breast, colorectal, gastric, lung, and prostate carcinomas. It is also observed in gliomas, melanomas, and osteoclastomas, which suggests that cathepsin B is involved in the development, invasion, and metastasis of several types of tumors (Koblinski et al, 2000).

Diagnosing a patient with a particular cancer, vascular disease, or inflammatory disorder can sometimes be determined by evaluating specific enzyme levels. This can be done through a variety of common serum blood tests. For example, detection of elevated levels of aspartate aminotransferase, alkaline phosphatase, 5' nucleotidase, and gamma-glutamyl transpeptidase are indicators of liver dysfunction (Reichling & Kaplan, 1988). However, due to the universal application of these tests, additional assays to anatomically

localize and quantitate enzyme levels in a patient may not seem feasible to conduct due to the limited knowledge gathered for prognosis. As further diagnosis, sometimes diagnostic methods such as tumor biopsy, exploratory surgery, site-directed radiation, and complete tumor dissection may be performed, but these can only be efficiently and safely performed when the precise location of the diseased tissue is known. Also, mRNA and proteomic screens can give insight to the enzyme activity within the body, but many enzymes are activated by post-translational processing which cannot be identified with these assays (Phizicky et al., 2003).

## **1.2 Enzyme-sensitive Fluorescent Probes *in vivo***

Magnetic resonance imaging (MRI) and positron emission tomography (PET) are common clinical imaging modalities used to detect enzyme activity. However, fluorescence-based methods are becoming more attractive for the noninvasive detection of enzymatic activities due to the high contrast, high sensitivity, and cost-effectiveness of the fluorescence imaging modality (Alander et al., 2012). Fluorescence-based methods are beneficial in assessing treatment effects after therapy because a patient can be imaged multiple times without radiation-induced side effects. Fluorescence-based imaging also allows the monitoring of multiple targets simultaneously during the same procedure because fluorescent molecules (fluorophores) have different spectral parameters (Bogdanov & Mazzanti, 2013). Currently, the only near-infrared (NIR) fluorophore approved by the FDA for clinical use is indocyanine green (ICG). It can be used as an IV-administered, non-specific, fluorescent contrast agent for applications in intraoperative angiography, and in tumor mapping and staging (Alander et al., 2012).

Fluorescence is a property of organic, biological, and inorganic nanoparticles in which electromagnetic energy is absorbed and creates an emission of light (Rao et al., 2007). The excitation light is typically of shorter wavelength (or higher energy) than the emission light—the optimal wavelength for excitation and emission ranges from 650-900 nm (Funovics et al., 2003). Fluorescence can be found naturally in some tissues, which is exploited in clinical applications such as endoscopy and surgery. Autofluorescence imaging is a routine use of fluorescence for clinical detection and diagnosis because it can detect natural tissue fluorescence emitted by collagen, flavins, and porphyrins. The presence of disease is measured by changes in the emission wavelength which alters with the metabolic state of a potentially infected tissue (Song et al., 2011). According to Funovics et al., the ideal fluorophore for *in vivo* imaging is described by:

1. A peak fluorescence close to 700-900 nm
2. High quantum yield (number of photons emitted per photon absorbed)
3. Narrow excitation/emission spectrum
4. Non-toxicity
5. Excellent biocompatibility, biodegradability, or excretability
6. Availability of monofunctional derivatives for conjugations
7. Commercial viability and production scalability for large quantities required for human use

With regards to detecting enzymatic activity, enzyme-sensitive fluorescent probes are designed to correlate the change in fluorescence state with the activity of the enzyme. Activation of a fluorescent probe by an enzyme transforms the previously “silent” non-fluorescent probe into a fluorescent one, which exhibits a change in emission wavelength from short to long. Several different macromolecular chemistries and configurations have been constructed to target specific diseases and their enzymatic systems. The strategies vary in the way that the fluorescence-generating substrate targets the enzyme (whether covalently or non-covalently), and how the substrate molecule is made silent

(quenched) in the non-activated state. For instance, fluorophores may be quenched due to collisional interactions with other molecules (dynamic quenching), by interaction with surface plasmons, or by closely positioned secondary fluorophores with non-covalent complexes (close quenching) (Bogdanov & Mazzanti, 2013). Furthermore, fluorophores can be turned on and off by modulation of their electronic characteristics via oxidation-reduction and other chemical reactions (Wesler et al., 2011).

### 1.3 Macromolecular Fluorescent Probes

During initial *in vitro* imaging studies of cells using macromolecules tagged with the amino-reactive fluorescent dye fluorescein isothiocyanate (FITC), a decrease in fluorescence intensity and lifetime was observed when the fluorescein fluorophore molecules were quenched after linking to serum albumin (Maeda et al., 1969). Yet, there was an increase of fluorescein emission intensity and lengthening of fluorescence lifetime in the cells after the uptake. Additional experiments with FITC-labeled L- and D-polylysine were performed to confirm that proteolysis was responsible for the increase in fluorescence intensity and lifetime. Unlike L-polylysine, D-polylysine is non-cleavable by cellular proteases and did not exhibit changes in fluorescence intensity or lifetime (Maeda et al., 1969). This important finding helped the future development of *in vivo* imaging methods using macromolecular fluorescent probes.

It has been discovered that fluorescence intensity and lifetime changes resulting from cleavage of the enzymatic macromolecular substrate are a direct result of conformational and chemical changes of the cleaved fluorescent product. Due to the chemical properties of polypeptides, if reactive groups within a polypeptide chain are positioned spatially close to one another, the covalent linking of fluorophore molecules to

these amino groups (particularly the N- $\epsilon$ -amino groups of lysines) will exhibit low fluorescence (Bogdanov & Mazzanti, 2013). Synthetic poly- and oligo-amino acids have conformational flexibility because of their occurrence in extended coil conformation at a pH above 8.5. This characteristic allows these molecules to interact with a variety of different dyes due to:

1. Higher overall number of accessible reactive groups
2. Increased mobility which facilitates the formation of transient or stable dye dimers

Fluorescent dye quenching with these linear and branched synthetic poly-amino acids is highly probable because of the facility of collisional interaction and the formation of non-fluorescent dye dimers (H- or J-dimers) or higher order aggregates (self-quenching). For electro-neutral and hydrophobic fluorophores such as NIR cyanine dyes, the formation of non-fluorescent aggregates is more common than for other fluorophores. Sulfation of cyanine dyes allow for more efficient water solubility, but do not hinder the development of non-fluorescent H-aggregates. This biochemical property of sulfated cyanines and other NIR fluorophores can aid in the designation of macromolecular imaging substrates because of the increase of solubility of macromolecules with fluorophore-linked side chains (Bogdanov & Mazzanti, 2013).

#### 1.4 Protected Graft Copolymers

Protected graft copolymers (PGCs) are covalent conjugates made up of a poly-L-lysine (PLL) backbone covalently grafted to carboxylated methoxypoly(ethylene glycol) (MPEG) side chains via the N- $\epsilon$ -amino groups of PLL. PGCs were specifically designed as a non-aggregating covalent macromolecular graft-copolymer conjugate (**Figure 1**)

(Bogdanov et al., 2012), which aids in reducing rapid elimination and immunogenicity of poly-L-lysine (Bogdanov & Mazzanti, 2013).

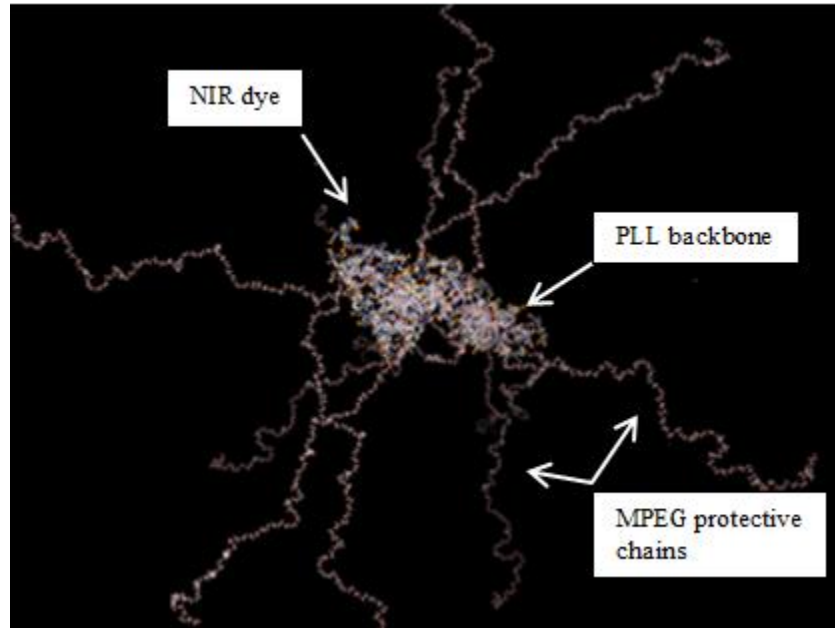


**Figure 1:** Molecular operating environment (MOE) illustrating the structure of PGC with a PLL backbone conjugated to a NIR dye (Bogdanov et al, 2012)

The MPEG esters linked to poly-amino acids help increase the hydrodynamic radius, which in turn increases circulation times of these imaging sensors *in vivo*. Defined as a long circulating agent, PGCs were first utilized as a carrier system for paramagnetic imaging compounds for MRI. For *in vivo* imaging of the bloodstream, PGCs allowed the imaging of localized morphological and functional abnormalities in the vascular system that resulted in recognition of local inflammation and visualized the blood supply of tumors (Bogdanov et al., 2012). Due to the high levels of water hydration and high segmental flexibility of PEGylation, the covalent linking of poly(ethylene glycol) (PEG) to other molecules, MPEG molecules can form a shell of “soft matter” around the PLL backbone which protects the linked backbone and fluorophores from rapid elimination in the bloodstream. In addition, PEG molecules

have the ability to protect biomacromolecules from activating immune responses (Bogdanov & Mazzanti, 2013).

The fluorophore-free state of MPEG-grafted PLL has a molecular mass of 350-450 kD, and can carry 50-55 amino groups per molecule. However, in the presence of cyanine dyes, not all amino groups can be modified due to steric constraints, and only 30-45 molecules of cyanine dyes can be linked per molecule of PGC. The background fluorescence of PGC dye-conjugated protease sensors is typically low in which the activation efficiency of the sensors depends on the following parameters:

1. Ability of the dyes to withhold a quenched state
2. Quantum yield of fluorescence in non-quenched state
3. Efficiency of backbone fragmentation by protease

These parameters vary depending on the NIR dye used; the spectral characteristics of the PGC dye-conjugate depends on dye density. For a PGC carrier linked to less than 12 dyes/molecule, the absorbance spectra depict minimal interaction between dyes. However, if there are more than 35 dyes/molecule, formation of an H-dimer can be observed through a distinct blue-shifted absorbance peak. The peak is not as pronounced after proteolytic cleavage of the probes. Cleavage also results in an increase of fluorescence intensity (Bogdanov & Mazzanti, 2013).

## **1.5 Macromolecular Fluorescent Probes in Cancer Imaging**

The main morphological hallmarks of cancer progression include:

1. Desmoplasia, the abnormal formation of fibroblast-like cells and extracellular matrix
2. Inflammation and immune responses, characterized by lymphocytes, macrophages, and dendritic cells
3. Angiogenesis, characterized by newly formed blood and lymph vessels

Cross-talk between cancer cells and stromal cells are mediated through direct heterotypic cell-cell interactions or by secreted molecules such as growth factors, cytokines, chemokines, extracellular matrix proteins, and proteases (De Wever & Mareel, 2003). For example, cancer cells generate a supportive microenvironment by producing stroma-modulating growth factors for fibroblast growth (bFGF), angiogenesis (VEGF and PDGF), extracellular protein ligands (EGFR), and interleukins. These factors interrupt normal tissue homeostasis, and function in a paracrine manner to stimulate stromal reactions. They also activate surrounding stromal cells types such as fibroblasts, smooth muscle cells, and adipocytes which secrete additional growth factors and proteases (Mueller & Fusenig, 2004). Proteases including MMPs, cathepsins, and uPA have been noted to accelerate the breakdown of the extracellular matrix and support cell migration and tumor angiogenesis (Kim et al., 1998). Cancer cells can initiate protease-dependent extracellular matrix modifications due to the interactions of mesenchymal and hematopoietic stromal cells, which allow malignant cells to penetrate the basement membrane and occupy neighboring tissues (Stetler-Stevenson et al., 1993).

Several fluorescence-based sensors have been developed for enzyme-mediated tumor detection via imaging proteolytic activity. Different probes are capable of detecting different targets of a tumor, giving specificity to the generated signal. Specifically, the PGC-fluorophore probes described earlier are capable of long circulation times in the bloodstream and can pass through highly permeable tumor vasculature to accumulate in tumors. When these probes are used to target intracellular enzymes, the cleaved fluorescent products are sequestered in the cells inside the solid tumor which allows the target-to-background ratio (the mean and maximum blood-normalized

standardized uptake value (Kim et al., 2010)) to increase, as the free probe and its associated background signal are removed from the body. These probes have also been designed to target extracellular enzymes such as MMPs, uPA, and thrombin (reviewed in Bogdanov & Mazzanti, 2013).

Administering PGC-fluorophore probes in tumor-bearing animals results in tumor-associated fluorescence intensity that is 12 times higher than the surrounding background. These probes are taken up via macropinocytosis by stromal cells that are recruited to the tumor microenvironments. These cells contain cysteine proteases, which are believed to activate the PGC-fluorophore probes (Bogdanov et al., 2002). Other such probes have been specifically designed to be activated by MMP, urokinase plasminogen activator, caspase-1, and coagulation enzymes. These PGC-fluorescent probe varieties are capable of imaging a broad spectrum of cancers in animal models including ovarian, colon, pancreatic, lung, fibrosarcoma, glioma, and metastatic disease (Bogdanov & Mazzanti, 2013).

Fluid-phase pinocytosis is an important process in which these PGC-fluorescent probe variants are taken up by the stromal cells. It is the uptake of solutes and membrane constituents by invaginations of the plasma membrane to create endocytic vesicles within the targeted cell. Pinocytosis of fluids can occur either through internalization of fluid by micro-pinocytosis (creating small vesicles called micro-pinosomes) or by macropinocytosis (creating large vacuoles called macro-pinosomes) (Buono et al., 2009). The formation of macro-pinosomes results in membrane ruffles folding back on the plasma membrane. This is observed in quiescent cells, and can be significantly increased by growth factors, phorbol esters, and diacylglycerol (Veithen et al., 1996).

Fluid-phase pinocytosis has been observed in stromal cells by measuring the amount of uptake of fluorescent dyes such as FITC-dextran. FITC-dextran is an ideal fluorescent dye conjugate to use due to its solubility in aqueous medium, membrane impermeability, stability within the intracellular environment, and lack of binding to the plasma membrane (Bar-Sagi & Feramisco, 1986). Experiments have also been performed using PGC labeled with NIRF dyes. The intracellular release of NIRF probes displays a fluorescent signal that can be identified *in vivo* at subnanomolar quantities and at depths adequate for experimental or clinical imaging (Tung et al., 2000).

PGC-fluorescent probes have been designed to detect tumor microenvironments of varying cancers after systemic administration, mainly as a result of cleaved fluorescent products accumulated in the extravascular compartment of solid tumors. However, the pathways and rates at which these probes are taken up and broken down by these microenvironments are still insufficiently investigated and poorly understood. This report will demonstrate the major characteristics underpinning the mechanisms of macromolecular poly-amino acid-based NIRF probe fragmentation by proteases and, consequently, the resultant time-dependent changes in fluorescence intensity of intracellular compartment and changes of cyanine dye fluorescence lifetimes.

## 2 Project Purpose

The detection of enzymatic activity in tissue stromal cells has proven to be beneficial in determining diagnosis and prognosis of a variety of diseases. Enzyme-sensitive PGC-fluorophore probes have been designed to detect tumor microenvironments when delivered *in vivo* through the bloodstream. Tumor microenvironments recruit and activate stromal cells for tumor invasion. However, the uptake and degradation pathways and rates at which these probes are catalyzed in a tumor microenvironment are still poorly understood. This MQP will investigate the mechanisms of PGC-based NIRF probe fragmentation via proteases. Assays will include monitoring time-dependent changes in fluorescence intensity of the intracellular compartment and changes of cyanine dye fluorescence lifetimes in these fluorescently tagged macromolecules.

### 3 Materials & Methods

#### 3.1 Synthesis of PGC Variants (NC, C1, C2)

Three different PGC variants were synthesized for the purpose of this project: Cleavable-1 (C1), Cleavable-2 (C2), and Non-Cleavable (NC) MPEG-g-PLL. Cleavable MPEG-g-PLL means that the bond between the PEG compound and the poly-L-lysine backbone can be cleaved by esterases, whereas, the bond cannot be cleaved in the non-cleavable MPEG-g-PLL. Original PGC products were provided by UMass Medical School in an aqueous phase. Samples were purified via six rounds of consecutive ultrafiltration in a centrifuge using YM50 cellulose membranes (0.1 M sodium chloride three times and deionized water three times). Half of the C1, C2, and NC PGC products were lyophilized for future use at  $-70^{\circ}\text{C}$ ; the rest was stored in liquid-form at  $-70^{\circ}\text{C}$ .

**Note:** For a majority of the experiments conducted for this project, NC PGC was used more than the other PGC variants. This is due to the fact that non-cleavable MPEG-g-PLL is more stable *in vitro* and in cells. The ester bonds in cleavable MPEG-g-PLL are sensitive to pH change and will cleave on their own under certain conditions.

#### 3.2 Synthesis of PGC-Fluorophore Probes

Five different PGC-fluorophore probes were synthesized for the purpose of this project—PGC variants were labeled with fluorescent dyes Alexa Fluor 488 and IRDye 680RD, 680FRED, 800CW, and 800RS NHS Ester Infrared Dyes. To synthesize the PGC-fluorophore probes, 30  $\mu\text{l}$  of PGC variant at 10 mg/ml concentration was incubated at room temperature in darkness for 1 hour with equivalent fluorescent dye concentrations corresponding to the amino group concentration of the particular PGC variant and 30  $\mu\text{l}$  0.1 M sodium bicarbonate (pH 8.6). (C1 PGC contained 5.25  $\mu\text{M}$   $\text{NH}_2$ ,

C2 PGC contained 1.9  $\mu\text{M}$   $\text{NH}_2$ , and NC PGC contained 4  $\mu\text{M}$   $\text{NH}_2$ —all at 10 mg/ml concentration). After incubation, samples were purified via centrifugation in Bio-Rad Bio-Spin 30 Chromatography Columns and stored at  $-20^\circ\text{C}$ .

**Note:** In early experimentation, Alexa Fluor 488 was used as a model for fluorescent dye interaction with MPEG-g-PLL due to its high quantum yield, water solubility, and inability to form micelles.

### 3.3 *In vitro* Cleavage and Fragmentation of PGC-Fluorophore Probes

Trypsin was used as a model for protease in the *in vitro* experiments. PGC-fluorophore probes were cleaved and fragmented using 0.1 mg/ml trypsin and left to incubate at room temperature for two different time points: 6 minutes and 12 minutes. Cleavage was also performed using immobilized trypsin. Immobilized trypsin was made by preparing 5 mL of ice-cold trypsin at a concentration of 10 mg/ml with 0.1 sodium tetraborate (pH 9.5) and adding 1 g of 1,1'-carbonyldiimidazole activated Novarose 1000/40 that was pre-washed in ice-cold deionized water. Solution was left to incubate on a rotary mixer at  $4^\circ\text{C}$  for 2 days. After incubation, the solution was washed with 0.1 M sodium chloride in a column. Standard and immobilized trypsins were used to compare which method would be more efficient to cleave the probes. To stop the reaction of the standard trypsin method, protease inhibitor TLCK was used, and the cleaved product was stored at  $-20^\circ\text{C}$ . For the immobilized trypsin method, the cleaved PGC sample was centrifuged and the supernatant was transferred into a tube and stored at  $-20^\circ\text{C}$ .

**Note:** Through experimentation, it was found that standard and immobilized trypsins cleave PGC-fluorophore probes at relatively the same efficiency. The standard trypsin

method was chosen over the immobilized trypsin due to the fact that immobilized trypsin began to degrade after a short amount of time when stored at 4°C. The standard trypsin method proved to be more reliable with long-term experimentation.

### **3.4 Gel Electrophoresis of *in vitro* Trypsin-Cleaved PGC-Fluorophore Probes**

When comparing trypsin methods for PGC-fluorophore probe cleavage, samples were run on an agarose gel at 50V for 20 minutes and then at 100V for 40 minutes. SDS-PAGE was conducted when the PGC-fluorophore probes were cleaved with only standard trypsin; the samples were run at 80V for 1.5 hours. The gels were imaged using UV illumination and were measured for green-fluorescence using a fluorescein filter/UVP Chemi Lab imaging device equipped with Hamamatsu CCD and for NIR fluorescence using an Odyssey gel reader (Li-Cor).

### **3.5 *Ex vivo* PGC-Fluorophore Probe Activation in Dermal Cells**

Human fibroblasts (Detroit 551 (ATCC® CCL-110™)) were cultured in Eagle's Minimum Essential Medium with L-glutamine and 10% fetal bovine serum (provided by ATCC). Human squamous carcinoma (A431) cells were cultured in Dulbecco's Modified Eagle Medium with L-glutamine and 10% fetal bovine serum (provided by Sigma-Aldrich). Both cell lines were grown in T75 flasks and seeded separately into an 8-well Lab-Tek® II Chamber Coverglass™ (approximately 10,000 cells per well). Once there was at least 70% confluency in each well of the two microchambers, the cells were incubated with PGC-fluorophore probes. For each microchamber, two wells were left without PGC-fluorophore probes to act as an experimental control, two wells were incubated with PGC-680RD, two wells with PGC-800CW, and two wells with PGC-

800RS. The microchambers were observed for probe uptake using an inverted fluorescence microscope at specific time points (2, 4, and 24 hours). For the purpose of all the *ex vivo* experiments, PGC-680RD probes were added to the cells at a dilution of 1:200 with respective media and PGC-800CW and -800RS probes were added to the cells at a dilution of 1:100 with respective media. Fluorescence intensity of NIR dyes was measured using Roper Scientific CCD controlled by IP LabSpectrum software (BD Bioscience) and a set of appropriate filters (Nikon).

### **3.6 Fluorescence Intensity and Lifetime Measurements of PGC-Fluorophore Probes**

Fluorescence intensity was calculated using IP LabSpectrum software for *ex vivo* activation of PGC-fluorophore probes. For *in vitro* activation, fluorescence intensity was evaluated by measuring changes of NIR fluorescence spectra using a Cary Eclipse or Spectramax M5 plate reader. Fluorescence lifetime was measured using a custom built time-domain imaging system equipped with a femtosecond Ti-Sapphire laser from Athinoula A. Martinos Center at Massachusetts General Hospital.

## 4 Results

The purpose of this project was to investigate the uptake and degradation of near-infrared long-circulating probes derived from methoxypoly(ethylene glycol)-grafted poly-L-lysine (MPEG-gPLL), similar to ProSense 750 (Perkin-Elmer). These probes, also known as protected graft copolymer (PGC), were examined under the conditions that model some aspects of tumor microenvironments. PGC-fluorophore probes are non-fluorescent unless they are cleaved, either chemically or enzymatically. The latter type of cleavage is typical if these probes are taken up *in vivo*. Experimentation was focused on the mechanisms of PGC-fluorophore probe fragmentation via proteases, time-dependent changes in fluorescence intensity resulting from the uptake in the intracellular compartments, and changes of cyanine dye fluorescence lifetimes of the fluorophores used for tagging PGCs.

### 4.1 Non-Random Cleavage of PGC-Fluorophore Probes

In order to demonstrate how proteases potentially cleave PGC-fluorophore probes in tumor microenvironments, probes labeled with Alexa Fluor (AF) 488 were cleaved with trypsin which acted as an *in vitro* model protease that would cleave PGC at the positions adjacent to free N- $\epsilon$ -amino groups of poly-L-lysine. Little is known about the way in which PGC-fluorophore probes are fragmented by multiple lysosomal cysteine proteases (e.g. cathepsins B, H, L, etc.) and was previously thought to occur randomly. To test this hypothesis, probes were exposed to trypsin at different time points in order to observe the potential timeframe needed for complete cleavage. Through gel electrophoresis, it was seen that trypsinization between time points 15-120 minutes was sufficient to fully cleave the probes (**Figure 2**). It was also observed that regardless of

the trypsin method used, the probes were consistently fragmented into distinct lengths. Lanes 2 and 3 were used as an undigested control to depict that non-cleaved C1 and C2 PGC-fluorophore probes are too large to travel down the length of the gel. The approximate fragment sizes of the cleaved bands detected were 67.2 kD, 53.9 kD, 38.8 kD, 23.2 kD, and 11.2 kD.

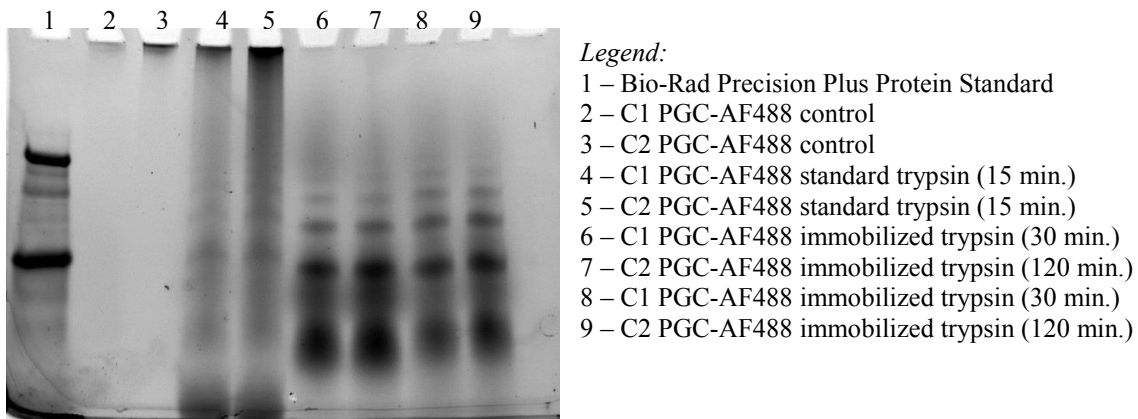


**Figure 2:** SDS-polyacrylamide gel illustrating *in vitro* trypsin-mediated fragmentation of C1 and C2 PGC-AF488 probes

Using only the standard trypsin method, PGC-800CW probes (i.e. the probes suitable for *in vivo* imaging) were cleaved at different time points to gauge which timeframe would be optimal for further experimentation. Probes were incubated for 0, 2, 3, 6, 12, and 24 minutes and one for 24 hours. **Figure 3** depicts the results observed via SDS-PAGE. It was observed that allowing trypsinization for 24 hours resulted in complete fragmentation of the probes, as evidenced by the lack of full-length probe at the top of the lane. The results obtained at time points greater than 6 minutes suggested that this time was sufficient for the appearance of a full range of fragmentation products and the first appearance of a completely cleaved PGC-fluorophore probe. Therefore, it was concluded that at the tested concentration of trypsin and its substrate (PGC-AF488), the

time point of 6 minutes was the shortest time sufficient for the reaction resulting in the full range of fragmentation products that were used for future experimentation.

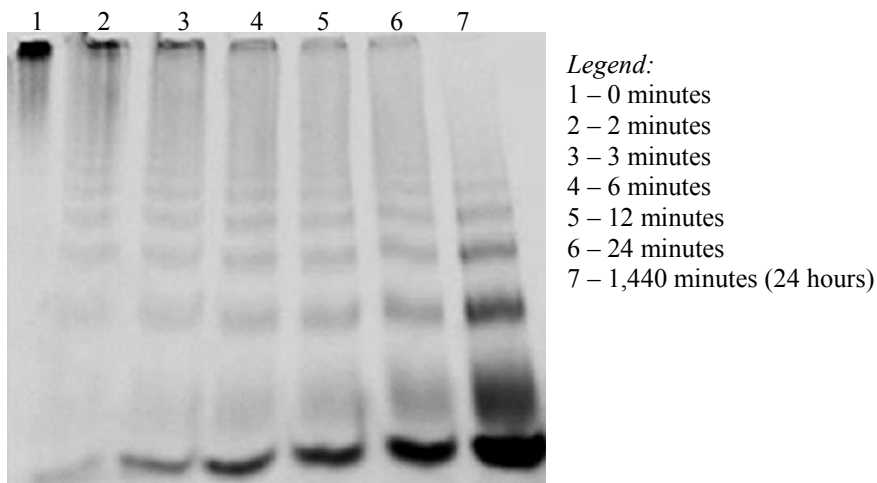


**Figure 3:** SDS-polyacrylamide gel illustrating the fragmentation of PGC-800CW probes by trypsin at different time points

Experimentation concerning the random cleavage hypothesis was also performed using PGC-680RD, -800CW, -800RS, and -800FRED probes with the standard trypsin method determined from **Figure 3**. Incubation of the probes with trypsin was either 6 or 12 minutes (**Figure 4**). Gel electrophoresis displayed the same fragmented lengths of the probe as observed in the previous figures (**Figures 2 and 3**). The lanes that were color-coded in green emitted fluorescence at a wavelength of 800 nm (800CW and 800RS) and the lanes color-coded in red emitted fluorescence at a wavelength of 700 nm (680 RD and 680FRED) (**Figure 4**). Lane 2 was used as a control to confirm that the non-cleaved NC PGC-fluorophore probes were too large to enter and travel down the length of the gel.

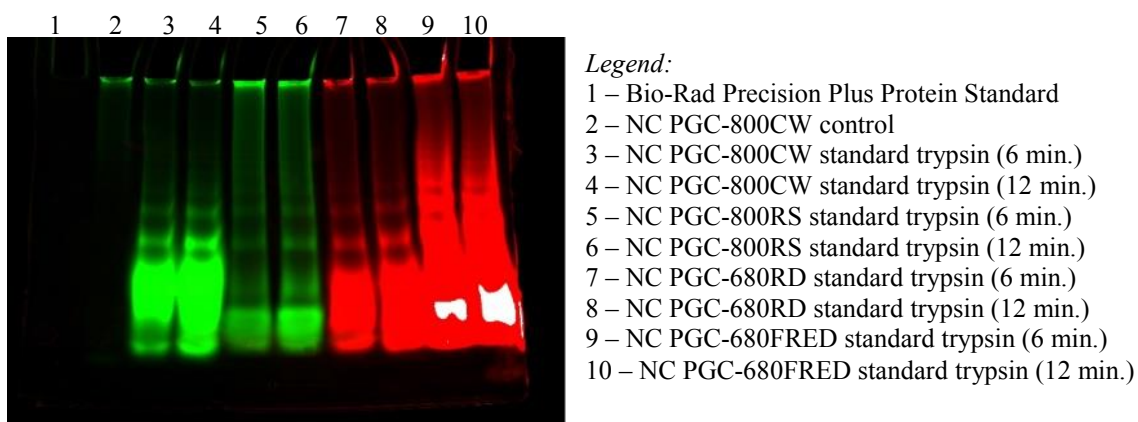


**Figure 4:** SDS-polyacrylamide gel illustrating *in vitro* trypsin-mediated fragmentation of NC PGC-680RD, -680FRED, -800CW, and -800RS probes

## 4.2 Fluorescence Intensity and Fluorescence Lifetime of Trypsin-Cleaved PGC-Fluorophore Probes

To investigate how trypsinization affects the fluorescence intensity (AU) of PGC-fluorophore probes, NIR fluorescence spectra were measured (**Table 1**). The table denotes the values gathered during experimentation with non-cleaved (controls, middle column) and cleaved NC PGC-AF488, -680RD, and -800CW probes (right column). It was observed that maximum fluorescence emission nearly doubled in value when NC PGC-fluorophore probes were cleaved by trypsin.

**Table 1:** Fluorescence intensity values of non-cleaved PGC-fluorophore probes (middle column) in comparison to trypsin-cleaved PGC-fluorophore probes (right column)

NC PGC-fluorophore probe type	Non-cleaved fluorescence intensity (AU)	Cleaved fluorescence intensity (AU)
AF488	1156.8	5162.6
680RD	48.158	71.55
800CW	23.536	40.465

The continuous wave (CW) fluorescence was measured at each fragment length of trypsin-cleaved PGC-800CW probes using the time-domain imaging system at Massachusetts General Hospital (**Figure 5**). CW signal imaging is a function of both fluorescence concentration and fluorescence lifetime (FL). FL imaging was also measured at each fragment length of the cleaved probe—FL reflects the fluorophore

microenvironment independently of concentration. The figure depicts the CW and FL maps of charge/mass separation (in nanoseconds) observed at each distinct fragment size. It was observed that the cleaved PGC-800CW probe (**Figure 5B**) undergoes a very rapid 1.5-fold increase in FL (within a minute) while the CW signal develops more slowly (on a scale of tens of minutes) (**Figure 5A**). By separating trypsin-cleaved fragments of PGC-800CW, it was observed that the fragmentation of probes quickly resulted in the larger, positively charged fragments having longer FL that predominated over the formation of the smaller, negatively charged fragments that had high fluorescence intensity but short FL.

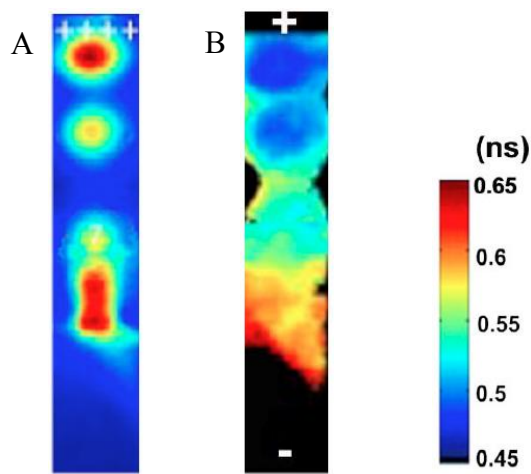


**Figure 5—Continuous Wave (CW) and Fluorescence Lifetime (FL) imaging of cleaved PGC-800CW probe:** (A) CW fluorescence concentration-dependent; (B) FL concentration-independent. Maps shows trypsin-cleaved PGC 800CW probes with highly fluorescent fragments slowly migrating to the cathode (large positively charged, long FL) and to the anode (small negatively charged, short FL).

### 4.3 Time-Dependent Fluorescence Intensity of PGC-Fluorophore Probe Activation in Cell Culture

In cell culture experiments, the PGC-fluorophore probe fragmentation was monitored by measuring near-infrared fluorescence in the intracellular vesicles. The imaging probes were incubated in the presence of sub-confluent human fibroblasts (D551) and human squamous carcinoma cells (A431), and fluorescence intensity changes in intracellular vesicles were measured over time. To obtain the mean fluorescence readings in individual vesicles, an image segmentation routine was applied by setting region-of-interest (ROI) limits using vesicle area descriptors which enabled the exclusion of noise (individual pixels), as well as large fluorescent artifacts originating from in-plane but out-of-focus cells. As a result, more than 100 data points were obtained from a single image and average fluorescence values were plotted over time. The fluorescence intensity values were corrected for background fluorescence that originated from the scattered excitation light. The uptake rates at which the cells internalized the probe were compared by using the emitted fluorescence measurements. The two cell lines tested (normal dermal fibroblasts and skin cancer cells) were monitored for fluorescence intensity changes at three time points: 2, 4, and 24 hours. The morphology of intracellular vesicles harboring near-infrared fluorescence can be found detailed in the Appendix section.

**Figure 6** and **Figure 7** depict the time-dependent fluorescence intensity changes observed during cell-mediated activation of PGC-680RD, -800CW, and -800RS probes in D551 and A431 cultures, respectively. It was observed that the NC PGC-680RD probes (blue curve) had a greater fluorescence intensity in both cell lines than the NC PGC-800CW and -800RS probes—the fluorescence intensity of the 680RD probes continued

to rapidly increase over time whereas the fluorescence intensity of the 800 dye probes increased at a much slower rate. When comparing the two cell lines, it can be seen that A431 cells uptake the PGC-fluorophore probes at a quicker rate than the D551 cells, and have overall greater fluorescence intensity. It should be noted that fluorescence signals measured in vesicles were very similar in their areas (ranging from 5.4-7.0  $\mu\text{m}$ ) in both cell lines. The overall vesicle area appeared to increase within 24 hours from 4.9 to 5.9  $\mu\text{m}$  in A431 cells, but in normal D551 cells decreased from 7 to 5.8  $\mu\text{m}$  (data not shown).

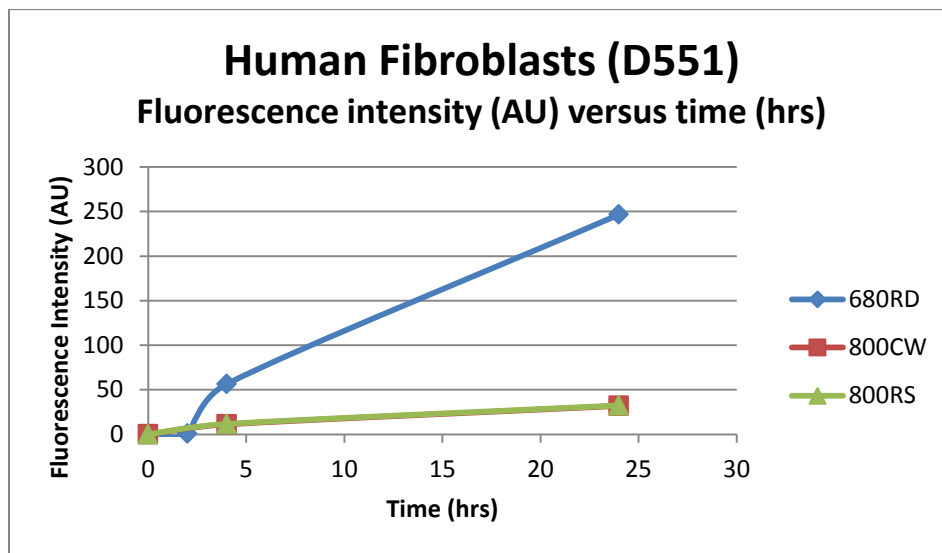


**Figure 6:** Fluorescence intensity over time in D551 cells seeded with NC PGC-fluorophore probes

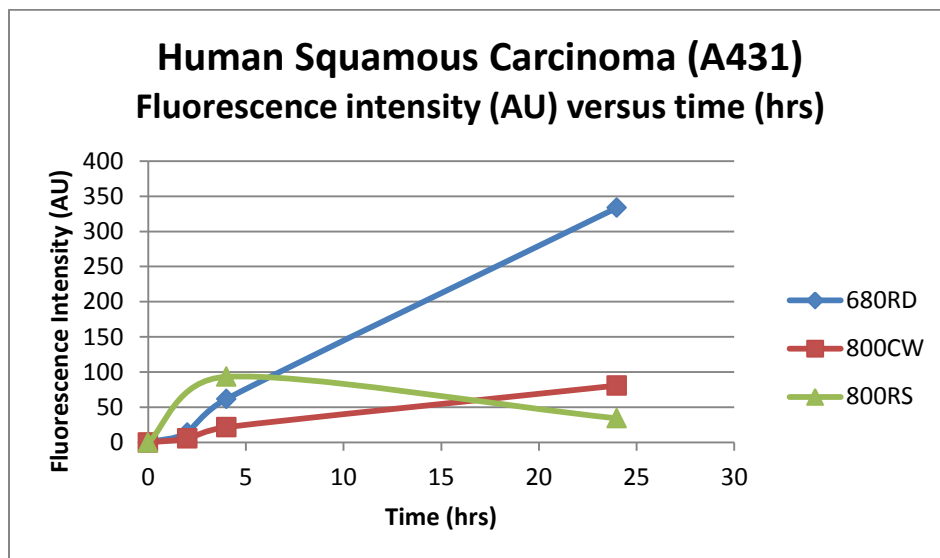


**Figure 7:** Fluorescence intensity over time in A431 cells seeded with NC PGC-fluorophore probes

## 5 Discussion

The data collected throughout the course of this project was in some ways novel and in other ways supporting of the ideas and concepts previously known about the uptake and degradation pathways of near-infrared long-circulating PGC-fluorophore probes in tumor-like environments. This project can be seen as a corridor to several supplementary projects which can specifically solidify the preliminary data presented in this report.

The first, and major, finding of the project rejected the original hypothesis that PGC-fluorophore probes due to random linking of both MPEG protective chains and fluorophores to the central backbone poly-amino acid should also be cleaved randomly by proteases. A model serine protease (trypsin) was used that has specificity similar to many lysosomal cysteine proteases (e.g. cathepsin B, H, L). This model protease was used for evaluating the hypothesis *in vitro* using various PGC variants (C1, C2, and NC) labeled with various types of fluorescent dyes (AF488, 680RD, 680FRED, 800CW, and 800RS). Regardless of the PGC-fluorophore probe type, cleavage with trypsin consistently resulted in distinct fragment sizes that were observed on gel electrophoresis (Figure 2). Trypsin accommodates small positively charged amino acid residues in its catalytic center and cleaves polypeptides (e.g. poly-L-lysine backbone) at the positions adjacent to free N- $\epsilon$ -amino groups. It was determined that the approximate molecular weights of each of the resultant fragments were the following: 67.2 kD, 53.9 kD, 38.8 kD, 23.2 kD, and 11.2 kD. Although the molecular weights of the tryptic fragments have been identified, it is unclear whether fluorescent properties of each of these fragment types are the same and whether trypsinolysis represents a good model of PGC-

fluorophore probe cleavage in the lysosomal compartment of cells. Additional experimentation to determine what those molecular weight sizes represent is needed to understand the exact mechanism of degradation that may occur *in vivo* with lysosomal cysteine proteases. Cleavage experiments using active recombinant purified cathepsins may prove beneficial as well to ensure consistency of approximated molecular weights with trypsin.

Next, the magnitude of fluorescence intensity increase and kinetics of fluorescence intensity changes were evaluated using trypsin-mediated cleavage of PGC-800CW probe. The reason NIR dye 800CW-modified PGC was chosen for these experiments were dictated by the fact that 800CW fluorescence can be potentially detected in deeper tissue due to the range of fluorescence light emitted by the dye and low toxicity of the dye (Bogdanov & Mazzanti, 2013). Both fluorescence intensity and fluorescence lifetime (FL) signals were monitored over time. Trypsinolysis of the PGC-800CW probe resulted in a rapid 1.5-fold increase in FL (within a minute) with a slower increase of intensity signal on a scale of tens of minutes (Figure 5). By using agarose electrophoresis, which resolves macromolecular mixtures by both charge and mass, it was observed that the larger positively charged probe fragments had a longer FL than the smaller negatively charged probe fragments that had high fluorescence intensity but short FL. These changes in fluorescence intensity and fluorescence lifetime are due to the conformational and chemical modifications that occur during proteolysis of the PGC-800CW probe. Polypeptides backbones such as poly-L-lysine in PGC exhibit low fluorescence intensities and short FL when fluorophores are linked to amino groups that are positioned spatially close to one another. When the peptide bonds in polypeptides are

cleaved by proteases (in this case, trypsin), fluorescence signal is increased due to the spatial separation of the fluorophores (Bogdanov & Mazzanti, 2013). Additional experiments involving imaging based on fluorescence intensity and FL of cell-mediated activation of PGC-800CW would be recommended to determine whether the same effects are observed *in vivo*.

Finally, the cell culture experiments showed a greater relative fluorescence intensity increase in cell-mediated activation of NC PGC-680RD probe than in NC PGC-800CW and -800RS probes (Figures 6 and 7). This was determined by performing CCD measurements of near-infrared fluorescence in intracellular vesicles of the human dermal fibroblast (D551) and human squamous carcinoma (A431) cell lines. In general, 2-dimensional cultures of fibroblasts and skin carcinoma cells engage in active uptake of the fluid phase (PGC-fluorophore probe mixed in cell culture medium). This beginning process of pinocytosis, or fluid phase uptake, takes less than a minute and cannot be observed with the PGC-fluorophore probes due to the fact that degradation has not occurred in cell vesicles (early endosomes). At later time points (4 and 24 hours), endosomes undergo acidification, maturation, and fuse with lysosomes which result in the initial probe degradation (Kallunki et al., 2013). Some of the contents of late endosomes undergo retro-endocytosis or slower exocytosis at later time points which results in an overall lower rate of accumulation of the markers of fluid-phase and, consequently, lower fluorescence (i.e. in the case of cell-mediated activation of PGC-800CW and -800RS) (Heeren et al., 1999).

In addition to fluorescence lifetime measurements, the vesicle area in which the fluorescence signal was assessed was also calculated to see if a trend could be found over

time. It was observed that the average fluorescent vesicle area was similar in both cell lines, however, there appeared to be an increase in vesicle area in the A431 cells but a decrease in the D551 cells over time—this indicates potential condensation of vesicles due to the differences in intracellular processing in the cancer and normal cell lines. This finding is consistent with frequently observed higher pinocytosis rates in cancer cells, but also suggests that the detection of cancer cells in the skin based on proteolysis of the long-circulating probes can be challenging due to a high rate of the same probe uptake in normal connective tissue cells. The observations also appears to be useful for explaining the presence of high near-infrared signal in the skin of animals injected with ProSense imaging probes, which are chemically similar to PGC-680RD and PGC-800CW probes used in this project (Bogdanov & Mazzanti, 2013). Further research is required to follow the uptake of a true fluorescent marker of the fluid phase (e.g. Lucifer Yellow CH) and fluorescent substrates for cathepsin B alongside PGC-fluorophore probes using multi-channel fluorescence acquisition.

## Bibliography

- Alander JT, Kaartinen I, Laakso A, Pätälä T, Spillmann T, Tuchin VV, Venermo M, and Välisuo P (2012) A Review of Indocyanine Green Fluorescent Imaging in Surgery. *International Journal of Biomedical Imaging*, **2012**: 940585.
- Bar-Sagi D, Feramisco JR (1986) Induction of Membrane Ruffling and Fluid-Phase Pinocytosis in Quiescent Fibroblasts by *ras* Proteins. *Science*, **233**: 1061-1068.
- Bogdanov AA, Mazzanti ML (2013) Fluorescent Macromolecular Sensors of Enzymatic Activity for *in vivo* Imaging. *Progress in Molecular Biology and Translational Science*, **113**: 349-387.
- Bogdanov AA, Lin CP, Simonova M, Matuszewski L, Weissleder R (2002) Cellular Activation of the Self-Quenched Fluorescent Reporter Probe in Tumor Micro-environment. *Neoplasia*, **4**: 228-236.
- Bogdanov AA, Mazzanti M, Castillo G, Elijah B (2012) Protected Graft Copolymer in Imaging and Therapy: A Platform for the Delivery of Covalently and Non-covalently Bound Drugs. *Theranostics*, **2**: 553-576.
- Buono C, Anzinger JJ, Amar M, Kruth HS (2009) Fluorescent Pegylated Nanoparticles Demonstrate Fluid-Phase Pinocytosis by Macrophages in Mouse Atherosclerotic Lesions. *The Journal of Clinical Investigation*, **119**: 1373–1381.
- De Wever O, Mareel M (2003) Role of Tissue Stroma in Cancer Cell Invasion. *The Journal of Pathology*, **200**: 429-447.
- Funovics M, Weissleder R, Tung C (2003) Protease Sensors for Bioimaging. *Anal Bioanal Chem*, **377**: 956-963.
- Heeren J, Weber W, and Beisiegel U (1999) Intracellular Processing of Endocytosed Triglyceride-Rich Lipoproteins Comprises Both Recycling and Degradation. *Journal of Cell Science*, **112**: 349-359.
- Kallunki T, Olsen OD, and Jäättelä M (2013) Cancer-Associated Lysosomal Changes: Friends or Foes. *Oncogene*, **32**: 1995-2004.
- Kim J, Yu W, Kovalski K, Ossowski L (1998) Requirement for Specific Proteases in Cancer Cell Intravasation as Revealed by a Novel Semi-quantitative PCR-based Assay. *Cell*, **94**: 353-362.
- Kim TN, Kim S, Yang SJ, Yoo HJ, Seo JA, Kim SG, Kim NH, Baik SH, Dong SC, Choi KM (2010) Vascular Inflammation in Patients with Impaired Glucose Tolerance and Type 2 Diabetes: Analysis with 18F-Fluorodeoxyglucose Positron Emission Tomography. *Circulation: Cardiovascular Imaging*, **3**: 142-148.

- Koblinski JE, Ahram M, Sloane BF (2000) Unraveling the Role of Proteases in Cancer. *Clinica Chimica Acta*, **291**: 113-135.
- Maeda H, Ishida N, Kawauchi H, Tsujimura K (1969) Reaction of Fluorescein-Isothiocyanate with Proteins and Amino Acids: I. Covalent and Non-Covalent Binding of Fluorescein-Isothiocyanate and Fluorescein to Proteins. *J. Biochem*, **65**: 777-783.
- Mueller MM, Fusenig NE (2004) Friends or Foes—Bipolar Effects of the Tumour Stroma in Cancer. *Nature Reviews Cancer*, **4**: 839-849.
- Pengfei L, Weaver VM, Werb Z (2012) The Extracellular Matrix: A Dynamic Niche in Cancer Progression. *J. Cell Biol.*, **196**: 395-406.
- Phizicky E, Bastiaens PIH, Zhu H, Snyder M, Fields S (2003) Protein Analysis on a Proteomic Scale. *Nature*, **422**: 208-215.
- Rao J, Dragulescu-Andrasi A, Yao H (2007) Fluorescence Imaging *in vivo*: Recent Advances. *Current Opinion in Biotechnology*, **18**: 17-25.
- Reichling JJ, Kaplan MM (1988) Clinical Use of Serum Enzymes in Liver Disease. *Digestive Diseases and Sciences*, **33**: 1601-1614.
- Song L, Banerjee S, Desilets D, Diehl DL, Farraye FA, Kaul V, Kethu S, Kwon RS, Mamula P, Pedrosa MC, Rodriguez SA, Tierney WM (2011) Autofluorescence Imaging. *Gastrointestinal Endoscopy Journal*, **73**: 647-650.
- Stetler-Stevenson WG, Aznavoorian S, Liotta LA (1993) Tumor Cell Interactions with the Extracellular Matrix During Invasion and Metastasis. *Annual Review of Cell Biology*, **9**: 541-573.
- Tung CH, Mahmood U, Bredow S, Weissleder R (2000) *In vivo* Imaging of Proteolytic Enzyme Activity Using a Novel Molecular Reporter. *Cancer Research*, **60**: 4953-4958.
- Veithen A, Cupers P, Baudhuin P, Courtoy PJ (1996) v-Src Induces Constitutive Macropinocytosis in Rat Fibroblasts. *Journal of Cell Science*, **109**: 2005-2012.
- Welser K, Adsley R, Moore BM, Chan WC, Aylott JW (2011) Protease Sensing with Nanoparticle Based Platforms. *Analyst*, **136**: 29-41.

## Appendix

The figures below illustrate examples of what could be seen under a fluorescent inverted microscope using near-infrared light at different time points. All fluorescence images were imaged using the same exposure time (0.5 seconds).

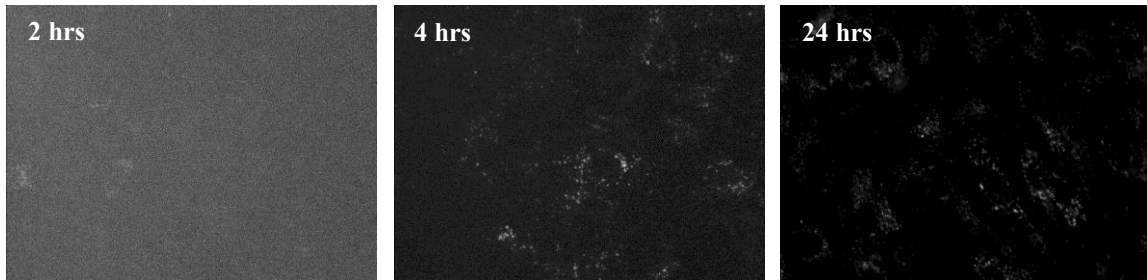


**Figure 8:** Fluorescence images of time-dependent NC PGC-680RD uptake into D551 cells

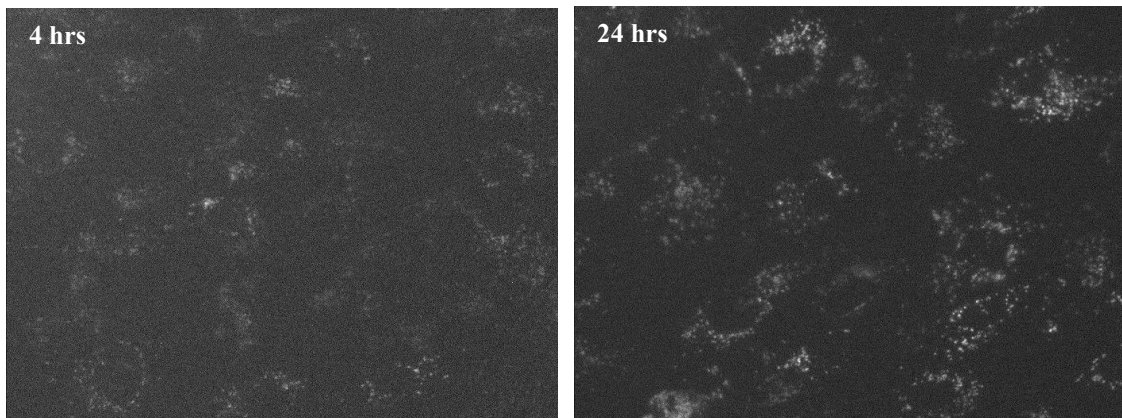


**Figure 9:** Fluorescence images of time-dependent NC PGC-800CW uptake into D551 cells

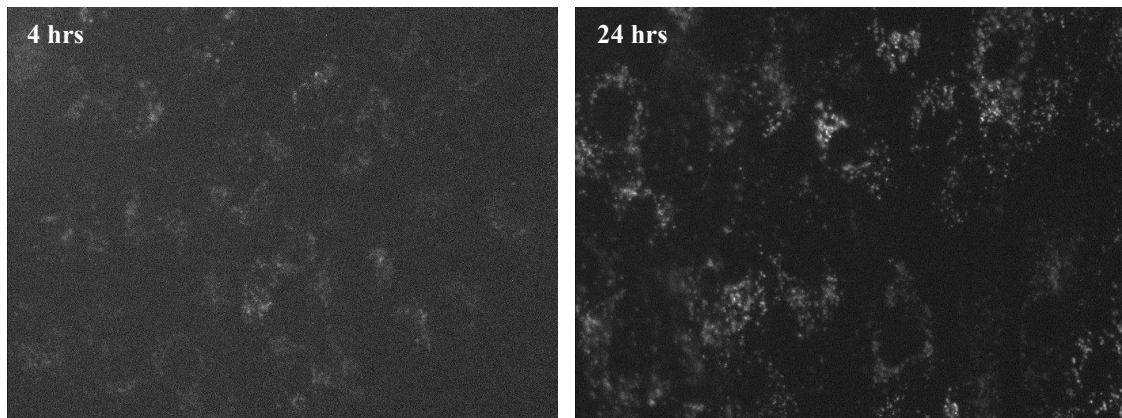


**Figure 10:** Fluorescence images of time-dependent NC PGC-800RS uptake into D551 cells

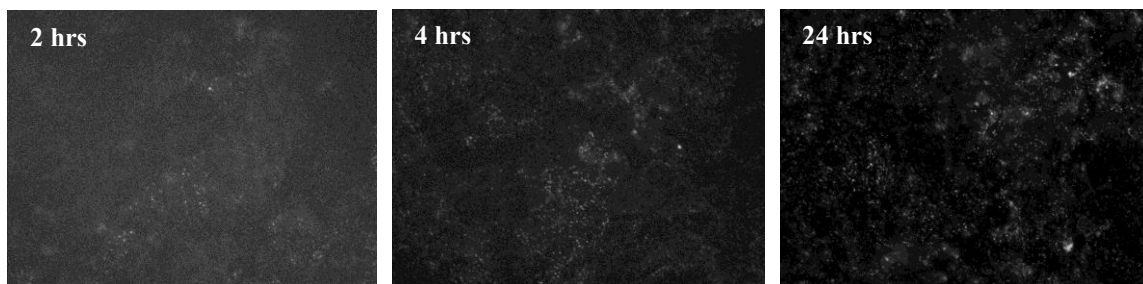


**Figure 11:** Fluorescence images of time-dependent NC PGC-680RD uptake into A431 cells

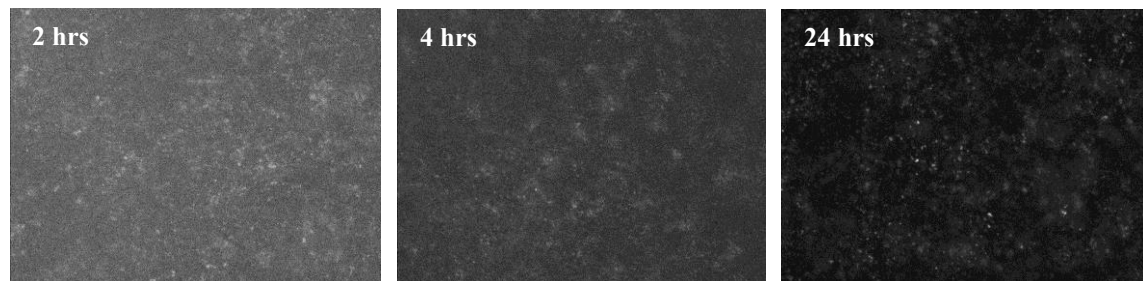


**Figure 12:** Fluorescence images of time-dependent NC PGC-800CW uptake into A431 cells

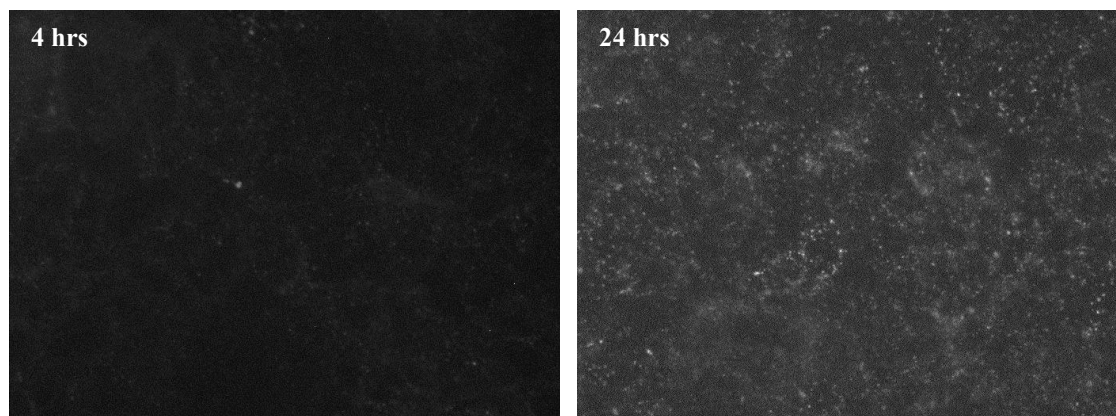


**Figure 13:** Fluorescence images of time-dependent NC PGC-800RS uptake into A431 cells